GNSS Integrity Enhancement for Urban Transport Applications by Error Characterization and Fault Detection and Exclusion (FDE)

Ni Zhu, David Betaille, Juliette Marais, Marion Berbineau

GEOLOCATION AND NAVIGATION
IN SPACE AND TIME

GNSS Integrity Enhancement for Urban Transport Applications by Error Characterization and Fault Detection and Exclusion (FDE)

Renforcement de l'Intégrité GNSS pour les Applications de Transport Urbain par Charactérization des Erreurs et la Détection et l'Exclusion des Défauts (FDE)

***Ni Zhu*[1], *David Bétaille*[2], *Juliette Marais*[1], *and Marion Berbineau*[3]**

[1] *Univ Lille Nord de France, IFSTTAR, COSYS, LEOST, F-59650 Villeneuve d'Ascq, France, {ni.zhu, juliette.marais}@ifsttar.fr*
[2] *IFSTTAR, COSYS, F-44344 Bouguenais, France, david.betaille@ifsttar.fr*
[3] *IFSTTAR, COSYS, F-59650 Villeneuve d'Ascq, France, marion.berbineau@ifsttar.fr*

Keywords: GNSS, integrity monitoring, FDE, urban environments
Mots-clefs: GNSS, la surveillance de l'intégrité, la détection et l'exclusion des défauts (FDE), l'environnement urbain

Abstract:
In the past decades, more and more Global Navigation Satellite Systems (GNSS)-based urban transport applications emerged. Among these applications, the liability critical ones, such as Electronic Toll Collection (ETC) and Pay as you Drive insurance, have high requirements for positioning accuracy as well as integrity since large errors can lead to serious consequences. Yet urban environments present great challenges for GNSS positioning due to the existence of multipath effects and None-Line-of-Sight (NLOS) receptions. This article presents a complete integrity monitoring scheme for urban transport applications. This scheme is realized in several levels. Firstly, measurement errors are better characterized by using weighting models with the help of an Urban Multipath Modeling (UMM). Secondly, several Fault Detection and Exclusion (FDE) methods are applied in order to detect and exclude erroneous measurements. Finally, Horizontal Protection Levels (HPLs) are computed and the probability of Misleading Information (MI) is analyzed.

Résumé:
Au cours des dernières décennies, de plus en plus d'applications de transport urbain basées sur les systèmes de positionnement par satellites (GNSS) ont vu le jour. Des applications exigent une fiabilité critique comme le télépéage basé sur l'utilisation du GNSS, pour lesquelles des erreurs de positionnement peuvent entraîner de graves conséquences. Pourtant, les environnements urbains présentent de grands défis pour le positionnement GNSS en raison de l'existence des trajets multiples et de signaux NLOS (None-Line-of-Sight). Cet article présente un système complet de surveillance de l'intégrité pour les applications de transport urbain. Tout d'abord, les erreurs de mesure sont mieux caractérisées en utilisant des modèles de pondération tirant parti d'un modèle de multi-trajet urbain (UMM). Deuxièmement, différentes méthodes de détection et d'exclusion de défauts (FDE) sont appliquées afin de détecter et d'exclure des mesures erronées. Enfin, les niveaux de protection horizontale (HPL) sont calculés et la probabilité d'événements redoutés (MI) est analysée.

1 Introduction

GNSS integrity is one criteria to evaluate GNSS performance, which was first introduced in the aviation field. It is defined as a measure of trust which can be placed in the correctness of the information supplied by the total system [1]. Since the complexity of urban environments, GNSS performance could be severely degraded if no special measures are taken. At the same time, the algorithms developed for the aerospace domain cannot be introduced directly to the GNSS land applications. This is because a high data redundancy exists in the aviation domain and the hypothesis that only one failure occurs at a time is made, which is not the case for urban users[2]. The main objective of this article is to present a complete integrity monitoring scheme for GNSS-based urban transport applications. With real data collected in urban environments, on the one hand, the measurement errors will be better characterized and reduced by different approaches. On the other hand, different FDE methods will be used in order to detect and exclude the faults. Finally, the HPL is calculated so as to provide a statistical position error bound.

The paper is organized as follows: After the introduction, two weighting models will be introduced: the C/N_0 (carrier-power-to-noise-density ratio) weighting model [3] and a new Hybrid model[4], which combines the C/N_0, the satellite elevation and an Urban Multipath Model (UMM), which is an improved version of the Urban Trench Model (UTM) described in [5]. In the next section, five different FDE method will be described briefly, including the Subset Test (ST) (also named exhaustive search), the Local Test (LT), the Forward-Backward (FB) Test, the Danish method as well as the Classic Test, [6][7]. Then, several HPLs will be discussed in order to choose the one which can better fit the urban canyons. The next section will present the real GPS data set as well as the evaluation of the accuracy performance with the Weighted Least Square (WLS) estimator compared to the Ordinary Least Square (OLS) estimator. Finally, five FDE algorithms will be applied with each WLS estimator and HPL will be calculated. The integrity performance will be analyzed from different aspects.

2 Error Characterizations: Signal Weighting

GNSS signals are often influenced by different error sources during the transmission in the propagation channels. Distributing different weights to each pseudo-range measurement according to the severity of its contamination is often an economic way to enhance the accuracy of positioning for the commercial GNSS receivers. This approach can be highly efficient if the propagation errors could be properly characterized. Conventional weighting models are often determined by signal transmission delay, such as ionospheric, tropospheric delay, etc, far from considering the real-time local effects, such as the multipath and NLOS reception. In fact, these local effects are predominant in the total GNSS measurement error budget for urban transport applications, since they can lead up to several kilometers' measurement error. In this paper, we will design the weighting matrix according to the real-time signal reception state.

Generally, the linearized GNSS pseudo-range observation equation can be written as:

$$\delta\rho = \mathbf{H} \times \delta x + \epsilon \tag{1}$$

where, $\delta\rho$ is the deviation between the actually measured pseudo-ranges and the predicted noiseless pseudo-ranges with a specified initial user state;
$\mathbf{H}$ denotes the geometry matrix in which describes the satellite-receiver relative position information;
δx represents the offset vector of the user states $(x, y, z, \delta t)$ with the initial states;
ϵ denotes the measurement error vector.

The Weighted Least Square (WLS) solution of δx is expressed as:

$$\delta x = [\mathbf{H}^T\mathbf{W}\mathbf{H}]^{-1}\mathbf{H}^T\mathbf{W} \times \delta\rho \tag{2}$$

here, $\mathbf{W}$ represents the measurement weighting matrix.

In fact, the weighting matrix $\mathbf{W}$ is a diagonal matrix, whose diagonal elements are the reciprocal of each variance of measurement as shown in Eq.3. That is to say, measurements with smaller error variances will contribute to larger weights in the estimation. On the contrary, measurements with larger error variances, such as NLOS signals, will get smaller weights or even approximately canceled from the measurement set by a nearly zero weight. Thus, in the following parts, error variance estimation according to different error models will be implemented in this matrix and the navigation solutions will be estimated with the WLS according to Eq. 2.

$$\mathbf{W} = \begin{pmatrix} \frac{1}{\sigma_1^2} & \cdots & 0 \\ \vdots & \ddots & \vdots \\ 0 & \cdots & \frac{1}{\sigma_m^2} \end{pmatrix} \tag{3}$$

2.1 C/N_0-based Weighting model

The carrier-power-to-noise-density ration, *i.e.*, C/N_0 represents the ratio of signal power and noise power per unit of bandwidth. It can be seen as an indicator of the signal quality. Several weighting models exist in literature using C/N_0 as criteria[3][8][9]. In this paper we will choose the model in [3], which is firstly build up for geodetic receivers. And the following formula of variance estimation was proposed for all types of receivers:

$$\sigma^2 = a + b \cdot 10^{-0.1 \times C/N_0} \tag{4}$$

where, a (in m^2) and b (in m^2Hz) are model parameters.

The two model parameters a and b strongly relate to the receiver characteristics and signal reception environments. Calibrations are needed according to specific datasets and receivers.

2.2 A new Hybrid model: Contribution of the Urban Multipath Modeling (UMM)

Despite its non-complicated implementation, the C/N_0 weighting model presents some drawbacks especially in dense urban canyons. On the one hand, constructive multipath interference leads to an increase in C/N_0, while destructive multipath interference leads to a decrease. Thus all signals with high C/N_0 do not possess high quality but they all contribute to a larger weight in the C/N_0 weighting model when calculating a position. Thus, we propose here a new hybrid model which is inspired by [4]. This model takes into consideration not only the C/N_0, but also the satellite elevation θ and a LOS/NLOS indicator k from the UMM. This model of measurement error variance can be written as:

$$\sigma^2 = k \times \frac{m \cdot 10^{-0.1 \times C/N_0}}{sin^2(\theta)} \tag{5}$$

where,

$$k = \begin{cases} 1 & if \quad LOS \\ 10 & if \quad NLOS \end{cases}$$

m is a multiplier for model calibration, which depends on receivers and environments.

The UMM is an improved version of the Urban Trench Model (UTM) described in [5]. Based on 3D map data, the UTM calculates the mask of satellite visibility and the additional pseudo-range distance due to signal reflections. An important hypothesis of UTM is that, the length of the streets is infinite, where comes from the model name "Urban Trench". In fact, this hypothesis is an approximation of the map geometry which fits well the reality when the vehicle is inside the homogeneous streets which have approximately the same geometric features as an example of a typical urban trench shown in Fig.1a. However, this assumption is no longer true especially in the no-homogeneous streets or the intersections as shown in Fig.1b.

(a) Inside a homogeneous street: a typical urban trench

(b) At an intersection area

Figure 1 – Example of two kinds of streets

In order to avoid the drawback of the UTM, the UMM is proposed while getting rid of the infinite length street assumption. The process is first to detect if any facade exists in every satellite azimuth, with a height enough to occult the corresponding satellite elevation. This initial step will identify LOS/NLOS satellites. Fig.2 shows an example of this step at a crossroad in the *Chaussée de la Madeleine* of Nantes: Fig.2a is an illustration with the information of digital map, where the polygons represent upside view of buildings. The red lines represent the directions of each received satellite azimuth. Fig.2b is the street view of the same location provided by Google Earth.

The next step is to examine every facade locally, to detect whether it could make a specular reflection with the occulted satellite previously identified. In this case, the final step is to check that no other facade may occult the reflected ray, whether in between the antenna and the impact point, or whether in between the impact point and the satellite. In case several facades exist with reflected rays, the one with the largest grazing angle (*i.e.*, the smallest angle of incidence) is preferred. Facades are regarded as vertical planes, with the height of the polygon they belong to. Fig.3 shows an illustration of this step provided respectively by digital map (Fig.3a) and the same location provided by Google Earth (Fig.3b). The green line represents a NLOS satellite signal which is reflected by a facade (in blue) and then received by the user.

Finally, the additional distances will be calculated for all the NLOS receptions according to the geometrical rules of specular reflection. These additional distances will be corrected when applying the hybrid error model.

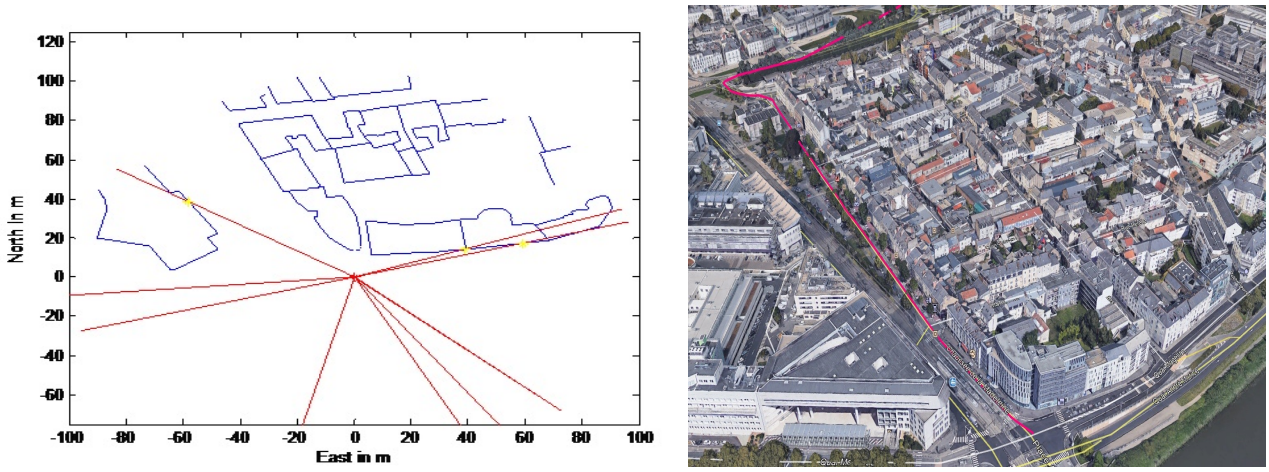

(a) (b)

Figure 2 – An illustration of the first step of the UMM

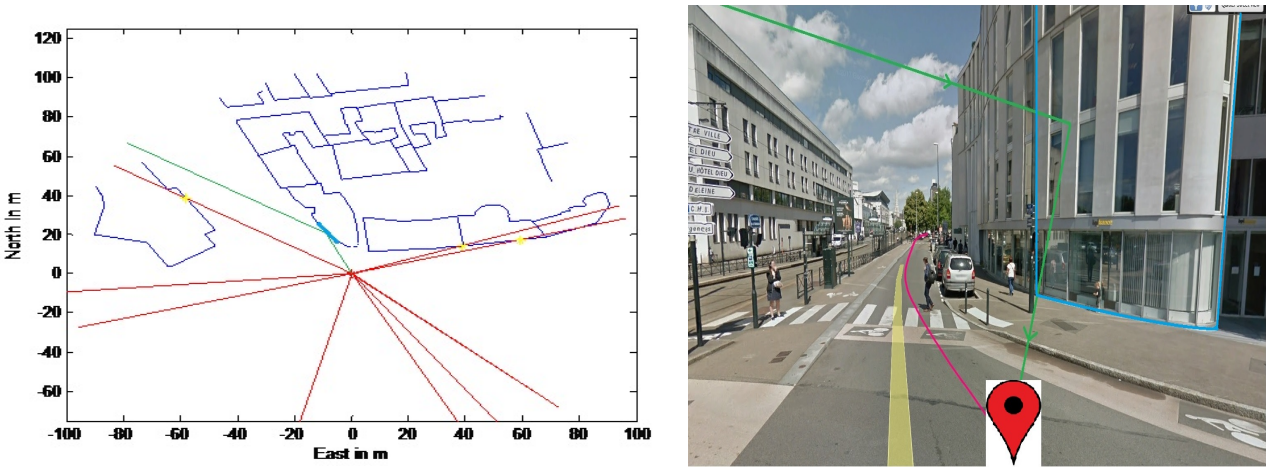

(a) (b)

Figure 3 – An illustration of the second step of the UMM

3 Fault Detection and Exclusion (FDE) Algorithms

Fault Detection and Exclusion (FDE) algorithms are generally based on the consistency check of the difference between the measured pseudorange ρ and the predicted pseudorange based on the estimated solution $\hat{x}$, which is called residuals. The WLS residual vector r can be written as:

$$\hat{r} = \delta\rho - H\delta\hat{x} \tag{6}$$

Two principle statistical hypothesis tests exist in FDE algorithms: the Global Test (GT) and the Local Test (LT). The GT is generally implemented at the primary stage in order to detect whether faulty measurements exist. And if a fault exists, the LT is able to further identify the faulty measurement.

3.1 Global Test

In the framework of the residual-based FDE, the test statistic t used in the GT is called Normalized Sum of Squared Error (NSSE), which can be expressed as:

$$t = \hat{r}^T \Sigma^{-1} \hat{r} \tag{7}$$

where, the matrix Σ denotes Variance Covariance Matrix (VCM) of measurements, which is also the inverse of the weighting matrix $\mathbf{W}$ mentioned previously in Eq.3.

Under fault-free conditions, the test statistic t follows a central χ^2 distribution; under faulty conditions, t follows a noncentral χ^2 distribution [10][11], which is illustrated in Fig.4a. With the pre-defined probability of false alarm P_{fa} and the probability of missed detection P_{md}, a threshold Th can be deduced and the statistical hypothesis test can be conducted as follows:

$$\begin{aligned} H_0 &: \text{(fault-free conditions)} \qquad t \leq Th \\ H_a &: \text{(faulty conditions)} \qquad t > Th \end{aligned} \tag{8}$$

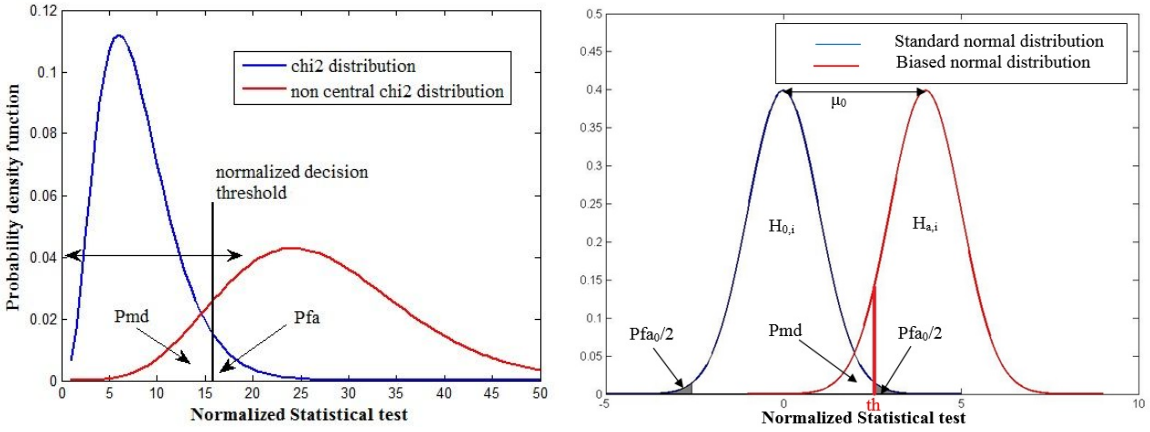

(a) Global Test (b) Local Test

Figure 4 – Global Test and Local Test

If the null hypothesis H_0 is rejected and the alternative hypothesis H_a is accepted, an inconsistency of the total measurement set is detected. Then, the fault identification procedure is needed to isolate and exclude the faulty measurement. The LT is one of methods to realize the fault identification.

3.2 Local Test

If a fault is detected with GT, that means an outlier exist in one or several measurements. LT can be carried out so as to identify the outlier. The LT uses the normalized residuals as test statistic, which can be written as follows:

$$w_i = |\frac{\hat{r}_i}{\sqrt{(C_{\hat{r}})_{ii}}}| \tag{9}$$

where, $(C_{\hat{r}})_{ii}$ represents the ith diagonal element of the covariance matrix of the residuals $C_{\hat{r}}$. The covariance matrix of residual is calculated as follows:

$$C_{\hat{r}} = \Sigma - H(H^T\Sigma^{-1}H)^{-1}H^T \tag{10}$$

If the ith measurement is not an outlier, w_i is supposed to follow a standard normal distribution, which is the local null hypothesis $H_{0,i}$. Otherwise, w_i follows a biased normal distribution, which corresponds to the local alternative hypothesis $H_{a,i}$ as shown in Fig.4b. In Fig.4b, th denotes the local threshold, which can be calculated with the predetermined local significance level P_{fa0}. As a result, the local test is realize as follows:

$$\begin{aligned} H_{0,i} &: \quad (i\text{th measurement not an outlier}) \qquad w_i \leq th \\ H_{a,i} &: \quad (i\text{th measurement an outlier}) \qquad w_i > th \end{aligned} \tag{11}$$

This procedure can be repeated several times in a loop until no outlier exists in current measurement set.

3.3 Different FDE Schemes

Different FDE methods exist by combining the GT and LT in different ways. In this paper, we will implement five FDE techniques which allow eliminating multiple faults. Most of them are explained in detail in our previous work [6]. So they will be briefly described here. In case of GT failure, the following FDE techniques can be carried out:

- Subset Testing (ST): each subset (number of satellite > 4) of the initial measurement set will be used to calculate an user position solution, among which the ST with the most satellites and the smallest test statistic which passes the GT will be chosen;
- Sequential Local Test (LT): each measurement will be examined by LT. In each iteration, the measurement with the biggest local test statistic exceeding the threshold will be eliminated as outlier. The procedure stops until no outlier exists or lack of redundancy;
- Forward-Backward (FB) Test: the forward loop will be conducted as the sequential LT described previously. Then in the backward loop, the eliminated satellites in the forward loop will be reintroduced with all the possible combination until the optimal measurement set is found. The main advantage of the FB technique is, on the one hand, to avoid the erroneous rejection of a good measurement since a huge measurement error can sometimes distribute and hide in other measurements' residuals due to special satellite geometry; on the other hand, the effect of re-introduction of previous excluded satellite can enhance the satellite geometry which is usually poor in urban canyon.
- Danish method (DAN): an iteratively reweighting procedure on the pre-estimated measurement variance will be carried out according to the ratio between local test statistic w_i and the local threshold th. What should be highlighted is that there is no exclusion step in this method, which can well keep the initial satellite geometry. If the algorithm cannot converge after several iteration (here, we fix it as 10), the solution will be declared as unreliable.
- The classic method: the measurement with largest normalized residual will be excluded in one iteration. The procedure stops until the GT passes or lack of redundancy.

During all the FDE procedures, if there is not enough redundancy to realize the FDE or the FDE cannot successfully identify the outliers, the position solution will be declared as unreliable.

4 Horizontal Protection Leval (HPL) Estimation

Protection Level (PL) is is a statistical error bound computed so as to guarantee that the probability of the absolute position error exceeding the said number is smaller than or equal to the target integrity risk[2][12]. Several methods of HPL computation exist in the literature especially for aviation utility. Generally speaking, a 'complete' HPL is composed of two terms: the impact of measurement noise on user position and the impact of measurement bias on user position. The noise term HPL_n is calculated according to the error propagation, which is defined in [12] as the HPL for Satellite-Based Augmentation System (SBAS):

$$HPL_n = K(P_{md}) \times d_{\text{major}} \tag{12}$$

where, d_{major} corresponds to the error uncertainty along the semi-major axis of the error ellipse. K is an inflation factor in order to meet specified integrity risk, which is usually obtained in the corresponding χ^2 table with 4 degree of freedom for conservative purpose. More details can be found in [12][13].

The noise term of HPL in Eq. 12 is often not big enough to bound the position errors especially in the presence of bias in one or several measurements. Thus, the bias term of HPL should be added. The bias term HPL_b generally consists of information of satellite geometry and the detectable bias in the domain of test statistic, which can be expressed as follows:

$$HPL_b(p_{bias}) = \max_i(SLOPE_i \cdot \sigma_i) \times p_{bias} \tag{13}$$

where,

$$SLOPE_i = \sqrt{\frac{(\mathbf{H}^+_{N,i})^2 + (\mathbf{H}^+_{E,i})^2}{\mathbf{S}_{ii}}} \tag{14}$$

with $\mathbf{H}^+ = (\mathbf{H}^T\mathbf{W}\mathbf{H})^{-1}\mathbf{H}^T\mathbf{W}$ and $\mathbf{S} = \mathbf{I} - \mathbf{H}\mathbf{H}^+$;
σ_i represents the standard deviation of the ith measurement;
p_{bias} denotes the bias in the domain of test statistic which can take different values according to the degree of conservative. This will be detailed in the following text.

In fact, $SLOPE$ represents the sensibility of HPE to the bias of ith satellite[13]. That is to say, the satellite with the largest $SLOPE$ is the most difficult to detect because given the same HPE, it yields the smallest test statistic. Also, given a test statistic, the satellite with the highest $SLOPE$ produces the largest position error.

Several variations of HPL_b exist by taking different values of p_{bias}, such as following cases:

- $p_{bias} = \sqrt{Th}$ [13], where Th represents the threshold of the GT which can be determined according to the predefined P_{fa};
- $p_{bias} = \sqrt{\delta}$ [14], where δ denotes the non centrality parameter in the non central χ^2 distribution described in Fig.4a;
- $p_{bias} = \sqrt{NSSE}$.

Finally, the complete HPL can be obtained as the sum of the noise term and the bias term:

$$HPL = K(P_{md}) \times d_{\text{major}} + \max_i(SLOPE_i \cdot \sigma_i) \times p_{bias} \tag{15}$$

The size of HPL is also an important issue for urban transport applications since it will be less effective if the size of HPL is too big compared to the size of current road where situated the user vehicle. Thus, a compromise should be made between the efficiency of the HPL (*i.e.*, HPL well bound the HPE) and its size.

In this paper, we will take $p_{bias} = \sqrt{NSSE}$. This is because: firstly, with the same integrity probability specifications and the same degree of freedom, we always have $Th < \delta$ which can be verified from χ^2 tables. Secondly, we can always make the GT pass after FDE so that $NSSE \leq Th$. As a result, by choosing $p_{bias} = \sqrt{NSSE}$, the HPL size can be well reduced. This is coherent with our results obtained from real data, in which the other two choices of p_{bias} often produce too big HPLs. Such conservative HPLs don't fit well with urban transport applications.

5 Application of the Complete Integrity Monitoring Scheme

5.1 Description of System and Dataset

The complete framework consists of two modules: an accuracy enhancement module and an integrity enhancement module as shown in Fig. 5. In the accuracy enhancement module, measurement errors will be characterized with error models mentioned in section 2. They will be compared with the results obtained from the Ordinary Least Square (OLS) estimator, in which, all the measurements have the same weight. Then, in the integrity enhancement module, five FDE methods mentioned in section 3 will be implemented and evaluated. In this paper, we fix $P_{fa} = P_{md} = 10^{-2}$. Finally, the HPL will be calculated according section 4.

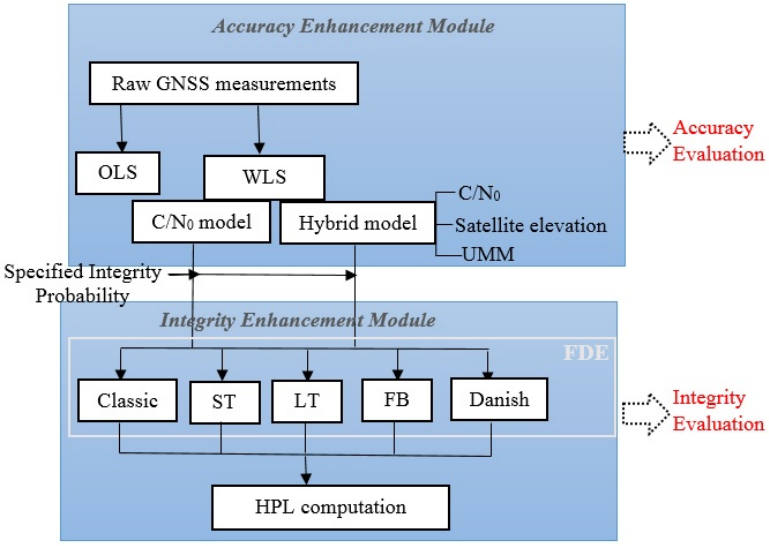

Figure 5 – An overview of the complete integrity monitoring scheme

The GPS data used to test the complete system was collected in the city center of Nantes, France. Two kinds of receivers are used: an Ublox-LEA-6T, which is a typical equipment used in car navigation systems and a dual-frequency Novatel-DLV3 receiver, which is a high precision receiver used to provide the reference trajectory. The total trajectory have 17903 epochs which takes about one hour at $5Hz$. Fig. 6 shows us an overview of this trajectory with Google Earth. We can see that the traveled streets are in deep urban canyons with different heights of buildings.

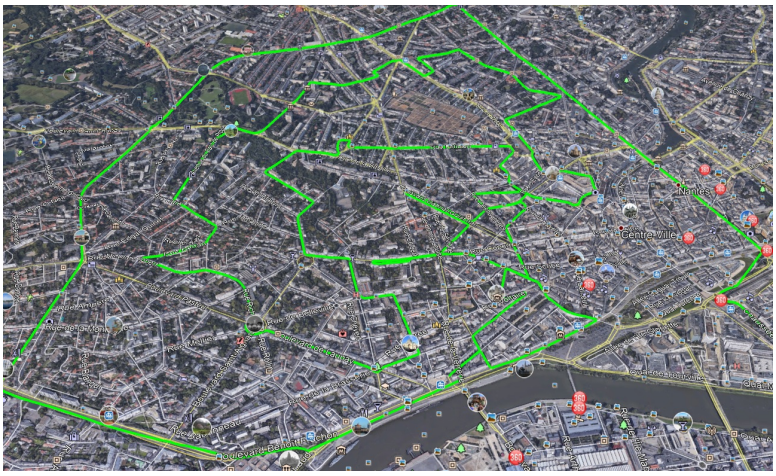

Figure 6 – An overview of the trajectory in the city center of Nantes, France

Horizontal Position Error (m)				
	Mean	Median	95%	std
OLS	10.14	5.66	30.74	77.39
WLS C/N_0	4.81	2.64	13.78	26.79
WLS Hybrid	3.61	2.33	10.83	4.43

Table 1 – WLS Accuracy Comparison (without FDE applied)

5.2 Experimental Validation and Performance Analysis

5.2.1 Performance of accuracy

In this sub-section, only the error models are applied (without FDEs). Fig. 7 shows the reference trajectory (in green) together with the trajectories estimated respectively by OLS (in blue), by WLS with C/N_0 model (in red of Fig. 7a) and by WLS with hybrid model (in red of Fig. 7b). Then Fig. 8 presents the Cumulative Distribution Function (CDF) of the HPE. We can see that with the two error models, the accuracy is well improved compared to the OLS, especially with the hybrid model. Table 1 makes a summary about the HPE in terms of mean, median (50^{th} percentile), 95^{th} percentile and standard deviation (std), which is used to evaluate the dispersion of HPE. We can see obviously that the WLS with hybrid model has the best performance concerning the accuracy. The main advantage of the hybrid model compared to the C/N_0 model is the capability of reducing huge errors since the 95^{th} percentile of HPE passes from 13.78m to 10.83m and the std passes from 26.79m to 4.43m.

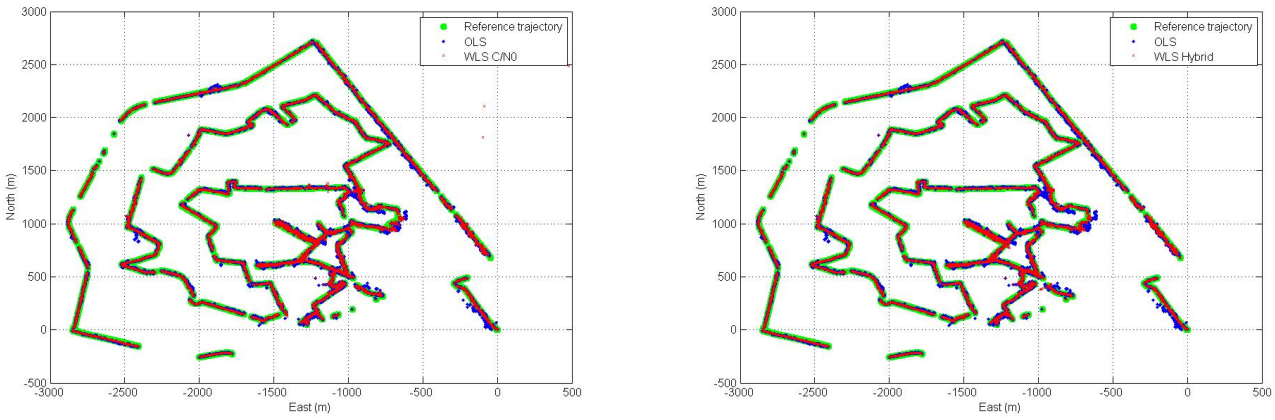

(a) (b)

Figure 7 – Comparison of Estimated Trajectories

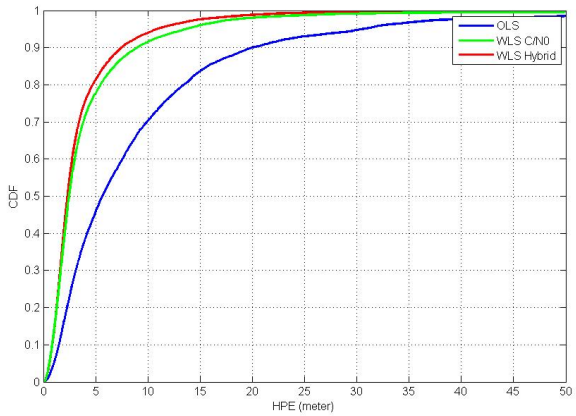

Figure 8 – Cumulative Distribution Function (CDF) of the HPE

	mean (HPE)	median (HPE)	95% HPE	std (HPE)	median(HPL)	Pmi
ST	4.61m	2.45m	14.44m	8.02m	18.26m	0.76%
LT	3.56m	2.38m	9.56m	4.41m	17.76m	0.11%
FB	3.43m	2.32m	9.90m	4.36m	17.46m	0.14%
DAN	4.13m	2.50m	11.18m	6.17m	19.21m	0.28%
Classic	4.55m	2.46m	13.61m	8.07m	18.29m	0.75%

Table 2 – Performance summary of C/N_0 model with FDE

5.2.2 Performance of integrity

After the accuracy enhancement, the integrity module is implemented and the HPL is calculated in this section. The main performance evaluated after application of FDE are mainly accuracy, the size of HPL as well as the efficiency of HPL. The last one is assessed by the probability of misleading information P_{mi}, which represents the probability of HPE exceeding HPL being the system declared the position solution is reliable.

Table 2 gives us a summary about the WLS with C/N_0 model with different FDE methods. We can see that the accuracy performance is again improved especially huge errors are removed since the standard deviations of HPE are much reduced. Among all the FDE methods, the FB has the best global performance and Fig. 9 presents some details. We can see in Fig.9a the reference trajectory (in green), the trajectory estimated with C/N_0 WLS (in sky blue) as well as the trajectory estimated with WLS C/N_0 and FB (the reliable positions are in magenta and unreliable positions are in black). Especially in the red circles, we can see that the majority of huge HPEs are either reduced or flagged as unreliable. All the P_{mi} are smaller than 1%.

Table 3 reports the performance of each FDE method with hybrid model. We can see that, with LT, FB and DAN, accuracy can be slightly improved compared to the one with only WLS hybrid model. Unfortunately, with ST and classic method, the accuracy is slightly degraded. Additional measures should be taken in the following research, such as special control of satellite geometry, in order to avoid this degradation. Compared to the performances of total integrity scheme with C/N_0 model, the sizes of HPL calculated with hybrid model are smaller. And all the P_{mi} can be guaranteed smaller than 1%.

As mentioned in Section 3.3, the FDE algorithms are not all the time available. When there is not enough

	mean (HPE)	median (HPE)	95% HPE	std (HPE)	median(HPL)	Pmi
ST	4.07m	2.39m	12.59m	6.34m	12.50m	0.95%
LT	3.42m	2.29m	10.59m	3.94m	12.36m	0.42%
FB	3.48m	2.28m	10.76m	4.03m	12.50m	0.48%
DAN	3.55m	2.30m	10.81m	4.67m	13.28m	0.21%
Classic	4.01m	2.39m	11.96m	7.16m	12.45m	0.80%

Table 3 – Performance summary of Hybrid model with FDE

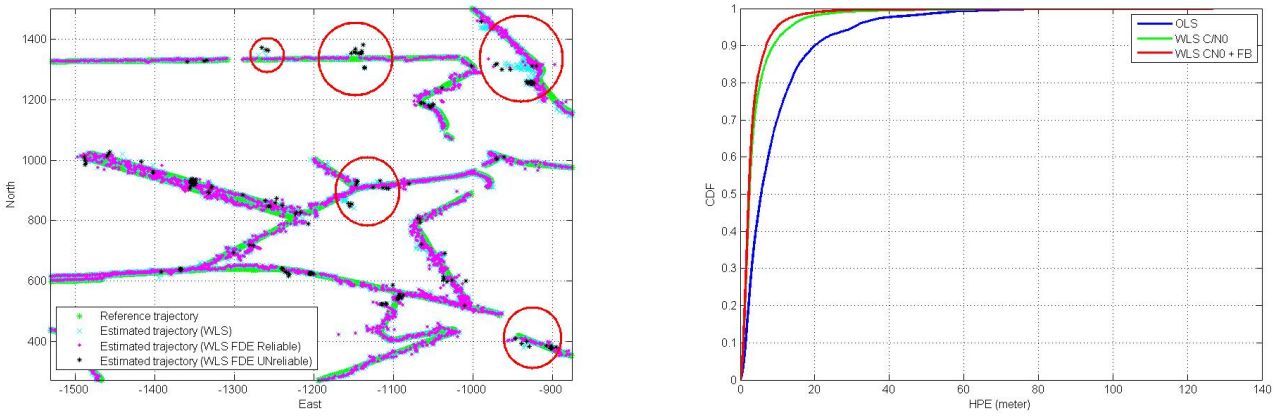

(a) A zoom of Estimated Trajectory

(b) CDF of HPE

Figure 9 – Performance of WLS C/N_0 with FB

(%)	ST	LT	FB	DAN	Classic
C/N_0	98.58	93.55	95.01	94.81	98.57
Hybrid	98.08	89.53	91.22	96.39	97.98

Table 4 – FDE Availability

redundancy to check the consistency or when the FDE algorithms are not able to identify the outlier, the system will be declared as non available. These positions will be flagged as unreliable. Table 4 reports the availabilities of each scheme. Thus, how to enhance the availability is also an issue for future research.

6 Conclusion

In this paper, we propose a complete integrity monitoring scheme for urban transport applications. This framework consists of two modules: one for accuracy enhancement, inside which, a new error model with the contribution of map information is proposed; the other for integrity enhancement, inside which, five FDE methods are implemented.

The validation with real GPS data collected in urban canyons shows that accuracy can be significantly improved by two error models compared to the classic Ordinary Least Square method especially the new hybrid model. All the FDE algorithms are able to help improve the accuracy of C/N_0 model but for hybrid model, only the Local Test, Forward-Backward Test and the Danish method can improve accuracy while the Subset Testing and the Classic method cannot due to satellite geometry degradation. Thus, special measures may be taken in order to avoid this degradation for future work. The HPL is able to well bound the HPE with P_{mi} smaller than 1%. HPLs still have a median value above 10 m in size (for HPE of 2 m in median), which is an issue to target for future research.

Acknowledgement

This work has been performed with the financial support of CNES and the Hauts de France Region Council in the framework of the SMARTIES project of the CPER ELSAT 2020 program which is co-financed by the European Regional Development Fund, the French state and the Hauts de France Region Council.

References

[1] P. B. Ober, *Integrity prediction and monitoring of navigation systems.* Integricom Publishers Leiden, 2003, vol. 1.

[2] N. Zhu, J. Marais, D. Bétaille, and M. Berbineau, "GNSS position integrity in urban environments: A review of literature," *IEEE Transactions on Intelligent Transportation Systems*, 2018.

[3] A. Wieser and F. K. Brunner, "An extended weight model for GPS phase observations," *Earth, planets and space*, vol. 52, no. 10, pp. 777–782, 2000.

[4] S. Tay and J. Marais, "Weighting models for GPS pseudorange observations for land transportation in urban canyons," in *6th European Workshop on GNSS Signals and Signal Processing*, 2013, p. 4p.

[5] D. Betaille, F. Peyret, and M. Ortiz, "How to enhance accuracy and integrity of satellite positioning for mobility pricing in cities: the Urban Trench method," in *Transport Research Arena TRA 2014*, PARIS, France, Apr. 2014, p. 8p, transport Research Arena TRA 2014, PARIS, FRANCE, 14-/04/2014 - 17/04/2014. [Online]. Available: https://hal.archives-ouvertes.fr/hal-01206082

[6] N. Zhu, J. Marais, D. Bétaille, and M. Berbineau, "Evaluation and comparison of GNSS navigation algorithms including FDE for urban transport applications," *Proceedings of ION ITM, Monterey, CA, USA*, 2017.

[7] H. Kuusniemi, A. Wieser, G. Lachapelle, and J. Takala, "User-level reliability monitoring in urban personal satellite-navigation," *IEEE Transactions on Aerospace and Electronic Systems*, vol. 43, no. 4, 2007.

[8] F. Brunner, H. Hartinger, and L. Troyer, "GPS signal diffraction modelling: the stochastic SIGMA-δ model," *Journal of Geodesy*, vol. 73, no. 5, pp. 259–267, 1999.

[9] H. Hartinger and F. Brunner, "Variances of GPS phase observations: the SIGMA-δ model," *GPS solutions*, vol. 2, no. 4, pp. 35–43, 1999.

[10] S. Kuang, *Geodetic network analysis and optimal design: concepts and applications.* Ann Arbor PressInc, 1996.

[11] A. Leick, L. Rapoport, and D. Tatarnikov, *GPS satellite surveying.* John Wiley & Sons, 2015.

[12] RTCA/DO-229D, "Minimum Operational Performance Standards for Global Positioning System/Wide Area Augmentation System airborne equipment," *RTCA SC-159*, 2006.

[13] T. Walter and P. Enge, "Weighted RAIM for precision approach," in *PROCEEDINGS OF ION GPS*, vol. 8. Institute of Navigation, 1995, pp. 1995–2004.

[14] R. G. Brown, *GPS RAIM: Calculation of Thresholds and Protection Radius Using Chi-square Methods; a Geometric Approach.* Radio Technical Commission for Aeronautics, 1994.